Alfredo R. de Faria
arfaria@ita.br
Instituto Tecnológico de Aeronáutica – ITA
12228-900 São José dos Campos, SP. Brazil

Prebuckling Enhancement of Beams and Plates under Uncertain Loadings and Arbitrary Initial Imperfections

Crooked beams and plates with arbitrary initial geometric imperfections are optimized in order to improve their prebuckling response in the presence of uncertain loadings. A novel optimization approach is presented to simultaneously handle the two types of uncertainties: arbitrary initial imperfection patterns and arbitrary loadings. A remarkable improvement in the prebuckling response of optimal designs is achieved by reducing the level of prebuckling displacements measured in some appropriate norm, irrespective of the uncertain imperfection pattern or loading. Two different norms are proposed, each one applicable to the beam or to the plate problem. The definitions of appropriate norms allow for the use of a minimax optimization approach that can consider the arbitrariness of both geometric imperfections and loadings. It is shown that the minimax procedure leads to optimum structural designs, in terms of optimal stiffness distribution, that are at the same time insensitive to perturbations in the loading space and to the pattern of initial imperfections in structure.
Keywords: optimization, uncertainty, convex modeling

Introduction

Real structures are not free of shape imperfections; a beam is slightly crooked, plates are not perfectly flat and shells exhibit similar deviations. In linear elastic analyses these imperfections (of small magnitude if compared to other dimensions of the structure) do not play a decisive role and can be neglected without detriment to the results. However, the shape imperfection effect is remarkable with respect to nonlinear stability theories.

Today it is a well-known fact that initial geometric imperfections can knock down the critical buckling loads of structures which possess a downwards secondary equilibrium path departing from the critical point (Koiter, 1945; Thompson and Hunt, 1973; Brush and Almroth, 1975; Roorda, 1986). Even when the post buckling equilibrium path does not turn downwards, as is the case with beams and plates, it is often required that initially imperfect structures remain as flat or undisturbed as possible under the application of in-plane loadings. Initial imperfections do not diminish the critical buckling load of beams or plates. However, in-plane compressive forces do magnify their effects and can possibly impair the overall behavior of the structure. As an example, skin panels comprising a control surface in an airplane should not present significant out-of-plane displacements when subjected to operation loadings not to compromise its aerodynamical performance.

Quantification of the initial imperfection effects in structures has been done (Adali, Richter and Verijenko, 1997; Hansen and Roorda, 1974; Tennyson, Chan and Muggeridge, 1971). These investigations were of utmost importance because real structures always present some level of imperfections due to fabrication. The difficulty is then to assess the imperfection patterns since some initial imperfections can be more harmful than others. Moreover, real structures are subjected to several load cases during operation and a particular imperfection pattern that is irrelevant for one load case may be highly relevant to another one. Hence, it is important to be able to predict not only the possible imperfection patterns but also to assess how each load case magnifies the effect of each imperfection pattern.

In this work an optimization procedure is proposed to improve the prebuckling response of crooked beams and plates with arbitrary initial geometric imperfections. Firstly, the crooked beam is presented to pose the problem in terms of formulation, applicable norms of prebuckling displacement and the maximization strategy proposed. The initial imperfection pattern is not known beforehand what complicates the optimization problem since one particular optimal design good for one type of imperfection may be bad for another one. The beam is acted upon by a compressive axial force denoted λ_0 and this is assumed to be the only applied load. From the governing equilibrium equations a procedure is proposed to handle the probable multiplicity of admissible imperfection patterns. Therefore, the beam problem is convenient as an introductory problem because of the simplification of admitting only one load case.

A plate with initial imperfections is the second model problem examined in this article. In this case three types of loadings are admissible: uniform normal loading in the x direction, uniform normal loading in the y direction, and uniform shear. Moreover, these three loadings may be applied individually or as a convex combination. For instance, 30% normal loading in the x direction, 20% normal loading in the y direction, and 50% shear loading. An optimization strategy is proposed where load ratios (0.3, 0.2 and 0.5) are variable but somehow limited by a constraint relationship. The initial imperfection pattern is not determined beforehand and the multiplicity of admissible loads (arbitrary convex combinations) only adds to the level of uncertainty involved. Nevertheless, it is shown that neither the variability of the load ratios nor the uncertainty related to the initial imperfections impede the optimization procedure from being highly efficient. Direct extension of the three load case problem is easily envisioned in order to accommodate virtually any number of load cases that might be of interest or necessity from the designer's point of view.

Beam Problem Formulation

Consider a simply supported crooked beam as shown in Fig. 1a where $w^*(x)$ is the imperfection pattern. It should be clear that the initial imperfections are exaggerated only to facilitate visualization. After a compressive load λ_0 is applied the beam develops out-of-plane displacements $w(x)$ as illustrated in Fig. 1b. The total potential energy Π associated with the beam can be written as (de Faria and Almeida, 1999):

$$\Pi = \frac{1}{2}\int_0^L D_{11} w_{,xx}^2 dx - \frac{\lambda_0}{2}\int_0^L w_{,x}^2 dx - \lambda_0 \int_0^L w_{,x} w_{,x}^* dx, \qquad (1)$$

Paper accepted August, 2007. Technical Editor: Nestor A. Zouain.

where D_{11} is the bending stiffness of the beam that can be used in the case of composite beams (assuming that the laminate is symmetric) (de Faria and Almeida, 1999). Equation (1) is the basis for a finite element discretization of the beam model. The global finite element matrix equations are

$$(\mathbf{K} - \lambda_i \mathbf{K}_G)\mathbf{q} = \lambda_0 \mathbf{K}_G \mathbf{q}^* \tag{2}$$

where $\mathbf{K}$ is the global stiffness matrix, $\mathbf{K}_G$ is the global geometric stiffness matrix, q is the global vector of displacements and $\mathbf{q}^*$ is the global vector of initial imperfections. It is clear that $\mathbf{K}$ and $\mathbf{K}_G$ correspond respectively to the first and second terms in Eq. (1). Matrix $\mathbf{K}$ depends of the thickness distribution of the beam and is independent of λ_0. On the other hand, matrix $\mathbf{K}_G$ is independent of both thickness distribution and λ_0. Notice that if $w^*(x)$ is available analytically, then it must be transformed into vector $\mathbf{q}^*$ through use of the element interpolation functions.

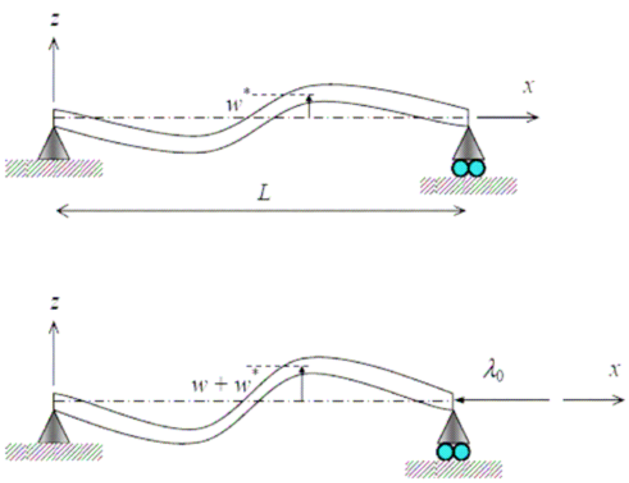

Figure 1. Crooked beam.

Solution of Eq. (2) yields vector $\mathbf{q}$. Moreover, the critical buckling load associated with the perfectly straight beam can also be obtained from Eq. (2) making $\mathbf{q}^* = \mathbf{0}$. This leads to the eigenproblem in Eq. (3) whose eigenpairs (buckling load, buckling mode) are $(\lambda_i, \boldsymbol{\phi}_i)$, $i = 1, 2, \ldots, n$, n being the total number of degrees of freedom in the finite element model.

$$(\mathbf{K} - \lambda_i \mathbf{K}_G)\boldsymbol{\varphi}_i = \mathbf{0} \tag{3}$$

Insight into the issue of a suitable norm for prebuckling displacements can be gained if $\mathbf{q}$ and $\mathbf{q}^*$ are spanned in the basis of buckling modes such that

$$\mathbf{q} = \sum_{i=1}^{n} a_i \boldsymbol{\varphi}_i \quad , \quad \mathbf{q}^* = \sum_{i=1}^{n} b_i \boldsymbol{\varphi}_i \tag{4}$$

where a_i and b_i are coefficients that can be computed noticing that the buckling modes are mutually orthogonal with respect to both $\mathbf{K}$ and $\mathbf{K}_G$. Hence, substitution of Eq. (4) into (2) leads to

$$a_i = \frac{\lambda_0}{\lambda_i - \lambda_0} b_i \quad \text{with} \quad b_i = \frac{\boldsymbol{\varphi}_i^T \mathbf{K}_G \mathbf{q}^*}{\boldsymbol{\varphi}_i^T \mathbf{K}_G \boldsymbol{\varphi}_i} \tag{5}$$

The issue of prebuckling enhancement requires the proposal of a norm to measure pre-buckling displacement. The prebuckling displacements depend on λ_0, however, let us λ_0 for a moment and return to this issue shortly. A possible norm consists in choosing one particular point on the beam and selecting the magnitude of its transverse displacement as a norm. This, however, can be misleading. For instance, suppose that the mid point of the beam is elected but the imperfection pattern is such that it matches exactly the second buckling mode of the simply supported beam. Assuming a constant thickness beam, from Eq. (5) it is concluded that, in this case $w^*(x) = \sin(2\pi x/L)$, $a_1 = 0$, $a_2 \neq 0$, $a_3 = a_4 = \ldots = 0$.

Moreover, from Eq. (5), $\mathbf{q} = a_2\boldsymbol{\phi}_2$, showing that the solution vector matches the second buckling mode which, in turn, has zero transverse displacement at the beam mid point.

A more comprehensive norm would be one that considers all response coefficients a_i simultaneously. This norm can be proposed as the maximum of all $|a_i|$ for all $i = 1, \ldots, n$ such that

$$\|\mathbf{q}\| = \max_i |a_i|. \tag{6}$$

The norm defined in Eq. (6) makes sense as long as the imperfection vector $\mathbf{q}^*$ is unique, i.e., if the imperfection pattern is known. However, that is not generally the case in real applications. Usually there is uncertainty associated with $\mathbf{q}^*$. Suppose that there may exist m ($m < n$) possible imperfection patterns $\mathbf{q}_1^*, \mathbf{q}_2^*, \ldots, \mathbf{q}_m^*$ that exist individually or as a convex combination of the form

$$\mathbf{q}^* = \sum_{j=1}^{m} \xi_j \mathbf{q}_j^*, \tag{7}$$

where $\xi_1, \xi_2, \ldots, \xi_m$ are arbitrary coefficients that satisfy

$$\sum_{j=1}^{m} |\xi_j| = 1. \tag{8}$$

The magnitude of the admissible imperfection patterns $\mathbf{q}_1^*, \mathbf{q}_2^*, \ldots, \mathbf{q}_m^*$ has an influence on the overall imperfection $\mathbf{q}^*$. Therefore, their magnitudes should not be too dispair. One way of guaranteeing equivalent magnitudes among $\mathbf{q}_1^*, \mathbf{q}_2^*, \ldots, \mathbf{q}_m^*$ is to make them equal to the buckling modes normalized with respect to the geometric stiffness matrix $\mathbf{K}_G$. Notice that m can be (and usually is) much smaller than n. Hence, the number of buckling modes used to represent the admissible imperfection patterns (m) is much smaller than the finite element model dimension (n).

In general, assume that the imperfection patterns are spanned by the buckling modes normalized with respect to matrix $\mathbf{K}_G$ such that

$$\mathbf{q}_j^* = \sum_{i=1}^{n} b_{ij} \boldsymbol{\varphi}_i \tag{9}$$

and, accordingly, the displacement vectors are

$$\mathbf{q}_j = \sum_{i=1}^{n} a_{ij} \boldsymbol{\varphi}_i \tag{10}$$

where, following Eq. (5),

$$a_{ij} = \frac{\lambda_0}{\lambda_i - \lambda_0} b_{ij}. \tag{11}$$

The "max" norm proposed in Eq. (6) must therefore be expanded to max $|a_{ij}|$ for all i = 1, …, n and for all j = 1, …, m. The following obvious inequality holds:

$$\max_{i,j}\left|a_{ij}\right| \geq \left|a_{kl}\right| \quad k=1,\ \ldots,\ n \quad l=1,\ \ldots,\ m. \tag{12}$$

Equation (12) can be multiplied by the positive number $|\xi_l|$ and summed up to yield

$$\begin{aligned}&\sum_{l=1}^{m}\left|\xi_l\right|\max_{i,j}\left|a_{ij}\right| = \left(\max_{i,j}\left|a_{ij}\right|\right)\left(\sum_{l=1}^{m}\left|\xi_l\right|\right) = \max_{i,j}\left|a_{ij}\right| \geq \\ &\sum_{l=1}^{m}\left|\xi_l\right|\left|a_{kl}\right| = \sum_{l=1}^{m}\left|\xi_l a_{kl}\right| \geq \left|\sum_{l=1}^{m}\xi_l a_{kl}\right|, \quad k=1,\ \ldots,\ n,\end{aligned} \tag{13}$$

where Eq. (8) has been employed. Notice that other relations involving the ξ_j's in Eq. (8) are also applicable. One could, for instance, adopt $\sum_{j=1}^{m}\xi_j^2=1$.

Since Eq. (13) is valid for all k = 1,…, n, it is particularly valid for

$$\max_{i,j}\left|a_{ij}\right| \geq \max_{k}\left|\sum_{l=1}^{m}\xi_l a_{kl}\right|. \tag{14}$$

Considering now an imperfection of the form given in Eq. (7), its associated displacement vector is

$$\mathbf{q} = \sum_{i=1}^{n}\frac{\lambda_0}{\lambda_i-\lambda_0}\left(\sum_{j=1}^{m}\xi_j b_{ij}\right)\boldsymbol{\varphi}_i = \sum_{i=1}^{n}\left(\sum_{j=1}^{m}\xi_j a_{ij}\right)\boldsymbol{\varphi}_i \tag{15}$$

Equations (15), (6) and (14) yield

$$\left\|\mathbf{q}\right\| \leq \max_{i,j}\left|a_{ij}\right|. \tag{16}$$

where $\mathbf{q}$ is a function of arbitrary ξ_j's as given by Eq. (15).

Equation (16) states that $\|\mathbf{q}\|$ is less or equal to max $|a_{ij}|$, even when an uncertain, arbitrary imperfection pattern of the form given in Eq. (7) exists. The equality sign in Eq. (16) holds when ξ_j = 1 and $\xi_1 = \ldots = \xi_{j-1} = \xi_{j+1} = \ldots = \xi_m = 0$. Therefore, from Eq. (16),

$$\max_{\xi_1,\ldots,\xi_m}\left\|\mathbf{q}\right\| \leq \max_{i,j}\left|a_{ij}\right|. \tag{17}$$

The conclusion reached in Eq. (17) can be used to advantage in an optimization procedure. Consider the problem of minimizing the prebuckling displacements of a crooked beam with constant mass where the imperfection patterns on that beam are uncertain. This uncertainty is reflected in the fact that there are m admissible imperfection patterns $\mathbf{q}_1$*, $\mathbf{q}_2$*, ..., $\mathbf{q}_m$* that may be applied separately or as a convex combination expressed in Eq. (7) with arbitrary ξ_1, ξ_2, ..., ξ_m that satisfy Eq. (8) or another equivalent constraint. This problem can be formulated as

$$\min_{\mathbf{h}}\max_{\xi_1,\ldots,\xi_m}\left\|\mathbf{q}\right\| \tag{18}$$

where $\mathbf{h}$ is a vector describing the thickness distribution. Within the finite element context $\mathbf{h}$ is the vector of nodal thicknesses. Expression (18) is a minimax problem (Demjanov and Malozemov, 1972). It provides simultaneously the best possible design against the worst possible combination of imperfection patterns.

In expression (18) a tremendous advantage has been gained from the fact that Eq. (17) holds. Actually, notice that expression (18) can be re-stated as

$$\min_{\mathbf{h}}\max_{\xi_1,\ldots,\xi_m}\left\|\mathbf{q}\right\| = \min_{\mathbf{h}}\max_{i,j}\left|a_{ij}\right| \tag{19}$$

Thus, the problem of maximizing $\|\mathbf{q}\|$ with respect to ξ_1, …, ξ_m can be replaced by the problem of finding the maximum $|a_{ij}|$, which is considerably simpler. A systematic procedure to find max $|a_{ij}|$ consists in, firstly extracting all the eigenpairs of the buckling problem stated in Eq. (3) and secondly computing all the aij from Eq. (5). Usually, obtaining *all* the eigenpairs of the buckling problem is not feasible. It is more practical to obtain a few buckling loads and modes corresponding to the lowest $|\lambda_i|$. The absolute value of λ_i is redundant in the beam problem since both the stiffness $\mathbf{K}$ and geometric stiffness $\mathbf{K}_G$ matrices are positive definite, which is easily inferred from their definitions in Eqs. (1) and (2). However, as will be shown in the plate case, negative eigenvalues may be present in the analysis.

The applied compressive loading λ_0 has been kept fixed up to now. The question of how the variation of λ_0 affects the proposed strategy can be elucidated if a graph of Eq. (5) is investigated. This is illustrated in Fig. 2 where a monotonically increasing function can be seen in the interval [0,1]. Hence, if λ_0 is decreased, it is certain that $|a_{ij}|$ also decreases for $0 \geq \lambda_0 < \lambda_i$. It is interesting to notice that, when $\lambda_0 < 0$, $|a_{ij}| < |b_{ij}|$, no matter how large $|\lambda_0|$ is. Physically it means that traction forces tend to alleviate the effect of initial imperfections.

Plate Problem Formulation

Consider a simply supported plate as shown in Fig. 3. Three types of loadings are applied to the plate: uniform normal loading in the x direction, uniform normal loading in the y direction, and uniform shear. These loadings are described in terms of two parameters: loading parameters denoted by R and a magnitude parameter denoted by λ_0. Different combinations of loading parameters may be applied indicating that there is uncertainty in the applied loadings. However, a constraint among them exists, namely,

$$\left|R_{xx}\right| + \left|R_{yy}\right| + \left|R_{xy}\right| = 1. \tag{20}$$

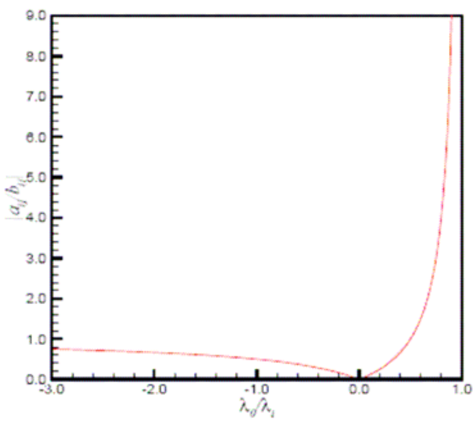

Figure 2. Response coefficients and variable loading.

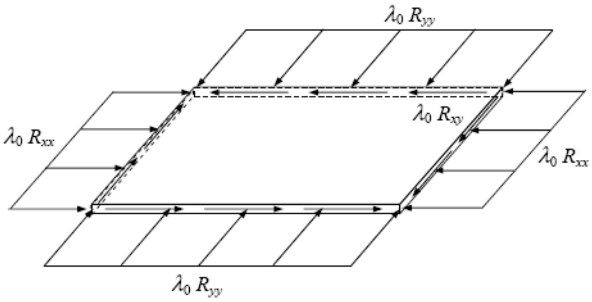

Figure 3. Plate with eligible loadings.

After a prebuckling load λ_0 is applied the plate develops out-of-plane displacements $w(x)$. The total potential energy Π associated with the beam can be written as (Brush and Almroth, 1975):

$$\Pi = \frac{1}{2}\int_\Omega \begin{Bmatrix} w_{,xx} \\ w_{,yy} \\ 2w_{,xy} \end{Bmatrix} \begin{bmatrix} D_{11} & D_{12} & D_{16} \\ D_{12} & D_{22} & D_{26} \\ D_{16} & D_{26} & D_{66} \end{bmatrix} \begin{Bmatrix} w_{,xx} \\ w_{,yy} \\ 2w_{,xy} \end{Bmatrix} d\Omega - \frac{\lambda_0}{2}\int_\Omega \left(R_{xx} w_{,x}^2 + R_{yy} w_{,y}^2 + 2R_{xy} w_{,x} w_{,y} \right) d\Omega - \lambda_0 \int_\Omega \left[R_{xx} w_{,x} w_{,x}^* + R_{yy} w_{,y} w_{,y}^* + R_{xy}\left(w_{,x} w_{,y}^* + w_{,y} w_{,x}^* \right) \right] d\Omega, \tag{21}$$

where the entries D_{ij} correspond to bending stiffnesses of a laminate plate, admitting a symmetric laminate (Daniel and Ishai, 2006). The global finite element matrices are therefore

$$(\mathbf{K} - \lambda_0 \mathbf{K}_G)\mathbf{q} = \lambda_0 \mathbf{K}_G \mathbf{q}^* \tag{22}$$

where

$$\mathbf{K}_G = R_{xx}\mathbf{K}_{Gxx} + R_{yy}\mathbf{K}_{Gyy} + R_{xy}\mathbf{K}_{Gxy} \tag{23}$$

and the geometric stiffness matrices $\mathbf{K}_{Gxx}$, $\mathbf{K}_{Gyy}$, $\mathbf{K}_{Gxy}$ are related to terms $\int w_{,x}^2 d\Omega$, $\int w_{,y}^2 d\Omega$, $\int 2w_{,x} w_{,y} d\Omega$, respectively.

Unlike the beam problem, a norm based on the coefficients a_{ij}, buckling loads λ_i and the buckling modes $\boldsymbol{\phi}_i$ is not convenient because it cannot be proved that a strong property given by Eq. (16) holds for all combinations of R_{xx}, R_{yy}, R_{xy}. An alternative norm to measure the prebuckling displacements is proposed as

$$\| \mathbf{q} \| = \frac{1}{2}\mathbf{q}^T (\mathbf{K} - \lambda_0 \mathbf{K}_G)\mathbf{q} \tag{24}$$

Notice that the norm defined in Eq. (24) satisfies the condition that it must be positive, provided $\mathbf{K} - \lambda_0\mathbf{K}_G$ is positive definite, what is always true if buckling has not occurred. This last claim may not seem so trivial because $\mathbf{K}_G$ may be indefinite. As a matter of fact, when shear loadings are applied, $\mathbf{K}_G$ is indefinite. A proof of this claim can be found in the work of de Faria and Almeida (2006).

The goal now is to prove that the norm defined in Eq. (24) is concave with respect to variations in the loading parameters. This can be done through a perturbation technique. When small perturbations δR_{xx}, δR_{yy}, δR_{xy} are imposed on the loading parameters the norm in Eq. (24) is also perturbed as in

$$\| \mathbf{q} \| + \delta \| \mathbf{q} \| + \delta^2 \| \mathbf{q} \| + ... = \frac{1}{2}(\mathbf{q} + \delta\mathbf{q} + \delta^2\mathbf{q} + ...)^T (\mathbf{K} - \lambda_0\mathbf{K}_G - \lambda_0 \delta\mathbf{K}_G)(\mathbf{q} + \delta\mathbf{q} + \delta^2\mathbf{q} + ...) \tag{25}$$

where

$$\delta\mathbf{K}_G = \delta R_{xx}\mathbf{K}_{Gxx} + \delta R_{yy}\mathbf{K}_{Gyy} + \delta R_{xy}\mathbf{K}_{Gxy} \tag{26}$$

In order to investigate the concavity of $\|\mathbf{q}\|$ it is important to study the sign of its second variation $\delta^2\|\mathbf{q}\|$. Thus, collecting second order terms in Eq. (25),

$$\delta^2 \| \mathbf{q} \| = \frac{1}{2}\delta^2\mathbf{q}^T (\mathbf{K} - \lambda_0\mathbf{K}_G)\mathbf{q} - \lambda_0 \delta\mathbf{q}^T \delta\mathbf{K}\mathbf{q} + \frac{1}{2}\delta\mathbf{q}^T (\mathbf{K} - \lambda_0\mathbf{K}_G)\delta\mathbf{q} \tag{27}$$

Simplification to Eq. (25) is obtained considering the perturbation of Eq. (22) that is

$$(\mathbf{K} - \lambda_0\mathbf{K}_G - \lambda_0\delta\mathbf{K}_G)(\mathbf{q} + \delta\mathbf{q} + \delta^2\mathbf{q} + ...) = \lambda_0(\mathbf{K}_G + \delta\mathbf{K}_G)\mathbf{q}^* \tag{28}$$

Equation (28) can be split into zero, first, second, etc. order terms as in

$$\begin{array}{ll} (\mathbf{K} - \lambda_0\mathbf{K}_G)\mathbf{q} = \lambda_0\mathbf{K}_G\mathbf{q}^* & \text{(zero order)} \\ (\mathbf{K} - \lambda_0\mathbf{K}_G)\delta\mathbf{q} = \lambda_0\mathbf{K}_G(\mathbf{q} + \mathbf{q}^*) & \text{(first order)} \\ (\mathbf{K} - \lambda_0\mathbf{K}_G)\delta^2\mathbf{q} = \lambda_0\delta\mathbf{K}_G\delta\mathbf{q} & \text{(second order)} \\ ... & \text{(higher order)} \end{array} \tag{29}$$

Substitution of the second order term of Eq. (29) into (27) leads to

$$\delta^2 \| \mathbf{q} \| = \frac{1}{2}\delta\mathbf{q}^T (\mathbf{K} - \lambda_0\mathbf{K}_G)\delta\mathbf{q} \tag{30}$$

The right hand side of Eq. (30) is positive if λ_0 is below the buckling load. Hence, $\delta^2\|\mathbf{q}\| \geq 0$. Since $\|\mathbf{q}\|$ is concave with respect to the loading parameters, maximization of $\|\mathbf{q}\|$ with respect to R_{xx}, R_{yy}, R_{xy} subjected to Eq. (20) is easily accomplished. It is sufficient to check, one at time, six load cases: (*i*) $R_{xx} = 1$ and $R_{yy} = R_{xy} = 0$, (*ii*) $R_{xx} = -1$ and $R_{yy} = R_{xy} = 0$, (*iii*) $R_{yy} = 1$ and $R_{xx} = R_{xy} = 0$, (*iv*) $R_{yy} = -1$ and $R_{xx} = R_{xy} = 0$, (*v*) $R_{xy} = 1$ and $R_{xx} = R_{yy} = 0$, and (*vi*) $R_{xy} = -1$ and $R_{xx} = R_{yy} = 0$. Actually, cases (*ii*) and (*iv*) do not have to be checked because $\mathbf{K}_{Gxx}$ and $\mathbf{K}_{Gyy}$ are both positive definite. Moreover, if an isotropic plate is considered, cases (*v*) and (*vi*) possess exactly the same eigenvalues. The highest $\|\mathbf{q}\|$ among cases (*i*), (*iii*) and (*v*) is the overall norm. Any convex combination of loading parameters is guaranteed to have a smaller norm.

The optimization problem posed is

$$\min_{\mathbf{h}} \max_{\xi_1,...,\xi_m, R_{xx}, R_{yy}, R_{xy}} \|\mathbf{q}\| \tag{31}$$

where the "max" part of the above expression is until here only partially solved since it was shown that $\|\mathbf{q}\|$ is concave with respect to the loading parameters. However, it remains to investigate what is the worst possible combination of ξ_1, ξ_2, ... ξ_m. In order to do it, assume that R_{xx}, R_{yy}, R_{xy} are fixed and the uncertain imperfection pattern is given by Eq. (7).

Moreover, the imperfection vector $\mathbf{q}_j^*$ is given by Eq. (9), and the associated displacements by Eq. (10). Substitution of Eqs. (7), (9) and (10) into Eq. (24) yields

$$\| \mathbf{q} \| = \frac{1}{2}\left[\sum_{i=1}^{n}\left(\sum_{j=1}^{m}\xi_j a_{ij}\right)\boldsymbol{\varphi}_i^T\right](\mathbf{K}-\lambda_0\mathbf{K}_G)\left[\sum_{k=1}^{n}\left(\sum_{l=1}^{m}\xi_l a_{kl}\right)\boldsymbol{\varphi}_k^T\right] \tag{32}$$

Simplification of Eq. (32) can be done recalling the orthogonality of $\boldsymbol{\phi}_i$. Notice, however, that $\mathbf{K}_G$ may be indefinite what leads to negative eigenvalues in the buckling problem. The orthogonalization relations are

$$\boldsymbol{\varphi}_i^T\mathbf{K}\boldsymbol{\varphi}_k = \begin{cases} 0 & \text{if} \quad i \neq k \\ -\lambda_i & \text{if} \quad 1 \le i = k \le s-1 \\ \lambda_i & \text{if} \quad s \le i = k \le n \end{cases}$$
$$\boldsymbol{\varphi}_i^T\mathbf{K}_G\boldsymbol{\varphi}_k = \begin{cases} 0 & \text{if} \quad i \neq k \\ -1 & \text{if} \quad 1 \le i = k \le s-1 \\ 1 & \text{if} \quad s \le i = k \le n \end{cases} \tag{33}$$

where

$$\lambda_1 \le \lambda_2 \le \ldots \le \lambda_{s-1} < 0 < \lambda_s \le \ldots \le \lambda_{n-1} \le \lambda_n \tag{34}$$

Substitution of Eq. (33) into Eq. (32) results in

$$\|\mathbf{q}\| = \frac{1}{2}\sum_{i=1}^{n}\left(\sum_{j=1}^{m}\xi_j a_{ij}\right)|\lambda_i - \lambda_0|\left(\sum_{l=1}^{m}\xi_l a_{il}\right). \tag{35}$$

Equation (35) can be recast into a more convenient form if two vectors are defined:

$$\boldsymbol{\xi} = \{\xi_1 \quad \xi_2 \quad \quad \xi_m\}^T \quad \text{and} \quad \mathbf{a}_i = \{a_{i1} \quad a_{i2} \quad \quad a_{im}\}^T \tag{36}$$

such that

$$\| \mathbf{q} \| = \frac{1}{2}\sum_{i=1}^{n}|\lambda_i - \lambda_0|\left(\sum_{j=1}^{m}\sum_{l=1}^{m}\xi_j\xi_l a_{ij}a_{il}\right) =$$
$$\frac{1}{2}\sum_{i=1}^{n}|\lambda_i - \lambda_0|\boldsymbol{\xi}^T(\mathbf{a}_i\mathbf{a}_i^T)\boldsymbol{\xi} = \frac{1}{2}\sum_{i=1}^{n}|\lambda_i - \lambda_0|\boldsymbol{\xi}^T\mathbf{C}_i\boldsymbol{\xi} = \frac{1}{2}\boldsymbol{\xi}^T\mathbf{C}\boldsymbol{\xi} \tag{37}$$

where $\mathbf{C}_i = \mathbf{a}_i\mathbf{a}_i^T$ and $\mathbf{C} = \sum_{i=1}^{n}|\lambda_i - \lambda_0|\mathbf{C}_i$. Notice that $\mathbf{C}_i$ is symmetric and positive definite and so is $\mathbf{C}$. The relationship involving ξ_1, ..., ξ_m is given by Eq. (8). Since $\mathbf{C}$ is positive definite it is certain that the norm expressed in Eq. (37) is a concave with respect to $\boldsymbol{\xi}$**.** Hence, the maximum value of $\|\mathbf{q}\|$ subjected to Eq. (8) is exactly the maximum value among the entries of $\mathbf{C}$ in its principal diagonal. This can also be mathematically argued. The positive definiteness of $\mathbf{C}$ allows one to write

$$(\boldsymbol{\xi}^T - \mathbf{e}_i^T)\mathbf{C}(\boldsymbol{\xi} - \mathbf{e}_i) \ge 0 \tag{38}$$

where $\mathbf{e}_i$ is the vector with ith component equal to unity and all the others zero. Considering that $|\xi_i| \ge \xi_i$, Eq. (38) can be multiplied by ξ_i to yield

$$|\,\xi_i\,|(\boldsymbol{\xi}^T\mathbf{C}\boldsymbol{\xi} + c_{ii}) \ge \xi_i(\boldsymbol{\xi}^T\mathbf{C}\boldsymbol{\xi} + c_{ii}) \ge 2\xi_i\mathbf{e}_i^T\mathbf{C}\boldsymbol{\xi} \tag{39}$$

where c_{ii} is the ith term of the principal diagonal of $\mathbf{C}$. Summing up Eqs. (39), recognizing that $\boldsymbol{\xi} = \Sigma\xi_i\,\mathbf{e}_i$, $c_{ii} > 0$ and using (8),

$$\sum_{i=1}^{m}|\,\xi_i\,|(\boldsymbol{\xi}^T\mathbf{C}\boldsymbol{\xi} + c_{ii}) = \boldsymbol{\xi}^T\mathbf{C}\boldsymbol{\xi} + \sum_{i=1}^{m}|\,\xi_i\,|\,c_{ii} \ge 2\boldsymbol{\xi}^T\mathbf{C}\boldsymbol{\xi} \Rightarrow$$
$$\boldsymbol{\xi}^T\mathbf{C}\boldsymbol{\xi} \le \sum_{i=1}^{m}|\,\xi_i\,|\,c_{ii} \le c_{MM} \tag{40}$$

where c_{MM} is the maximum of all c_{ii}, for $i = 1; \ldots, m$.

The optimization procedure in the plate case is:

- Solve three buckling problems $(\mathbf{K} - \lambda_i\mathbf{K}_G)\boldsymbol{\varphi}_i = \mathbf{0}$ associated with loading parameters labelled as cases (i), (iii) and (v);
- for each of these three cases find the prebuckling displacement vectors from $(\mathbf{K} - \lambda_i\mathbf{K}_G)\mathbf{q}_j = \lambda_i\mathbf{K}_G\mathbf{q}_j^*$ and related a_{ij};
- form matrices $\mathbf{C}_i$, $\mathbf{C}$ and obtain c_{MM};
- among the three c_{MM}'s obtained, the largest one is taken as $\|\mathbf{q}\|$.

Subsequently, proceed with the “min" part of the problem. A word of caution is worth giving regarding the “min" optimization problem: a method based on gradients is not recommended because the objective function involved comes from a maximization problem and, therefore, its derivatives may be highly discontinuous what leads to serious convergence difficulties. Therefore, the numerical optimization method selected to solve the “min" problem in this work is the Powell's method (Powell, 1964).

The question of whether the norm defined in Eq. (24) increases or decreases with λ_0 can be answered by taking its first derivative:

$$\frac{\partial \| \mathbf{q} \|}{\partial \lambda_0} = \left(\frac{\partial \mathbf{q}}{\partial \lambda_0}\right)^T(\mathbf{K} - \lambda_0\mathbf{K}_G)\mathbf{q} - \frac{1}{2}\mathbf{q}^T\mathbf{K}_G\mathbf{q} \tag{41}$$

where, in view of Eq. (2),

$$(\mathbf{K} - \lambda_0\mathbf{K}_G)\frac{\partial \mathbf{q}}{\partial \lambda_0} = \mathbf{K}_G(\mathbf{q} + \mathbf{q}^*) \tag{42}$$

Substituting Eq. (42) into (41),

$$\frac{\partial \| \mathbf{q} \|}{\partial \lambda_0} = \left(\frac{\partial \mathbf{q}}{\partial \lambda_0}\right)^T(\mathbf{K} - \lambda_0\mathbf{K}_G)\mathbf{q} - \frac{1}{2}\mathbf{q}^T\mathbf{K}_G\mathbf{q} =$$
$$(\mathbf{q} + \mathbf{q}^*)^T\mathbf{K}_G\mathbf{q} - \frac{1}{2}\mathbf{q}^T\mathbf{K}_G\mathbf{q} = \frac{1}{2}\mathbf{q}^T\mathbf{K}_G\mathbf{q} + \frac{1}{\lambda_0}\mathbf{q}^T(\mathbf{K} - \lambda_0\mathbf{K}_G)\mathbf{q} = \tag{43}$$
$$\frac{1}{\lambda_0}\mathbf{q}^T\left(\mathbf{K} - \frac{\lambda_0}{2}\mathbf{K}_G\right)\mathbf{q} = \frac{1}{2\lambda_0}\mathbf{q}^T(\mathbf{K} - \lambda_0\mathbf{K}_G)\mathbf{q} + \frac{1}{2\lambda_0}\mathbf{q}^T\mathbf{K}\mathbf{q}$$

Numerical Examples

The numerical examples intend to compare the prebuckling behavior of a variable thickness beam and a variable thickness plate before and after optimization. They also provide some ideas for code implementation and the give a few details on the numerical methods and elements used to solve the structural problems. In all examples presented the optimization procedure is carried out in two steps: 50,000 random designs are generated and the best one is selected as the starting point for a Powell's search.

The Beam Example

Consider a beam that has variable thickness and an arbitrary number of elements. Figure 4 illustrates such a beam modeled with eight elements, nine nodes and piecewise linear thickness distribution. The thicknesses need not to be defined at every node. In Fig. 4 they are defined at nodes 1, 3, 5, 7 and 9. Thicknesses at nodes 2, 4, 6 and 8 are obtained through linear interpolation of t_1 and t_2, t_2 and t_3, t_3 and t_4, and t_4 and t_5, respectively.

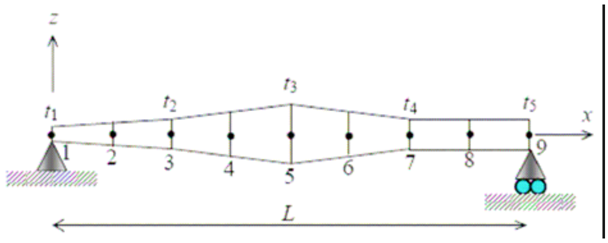

Figure 4. Variable thickness beam.

The element used is the traditional Euler-Bernoulli beam element with two nodes, two degrees of freedom per node, rectangular cross section and Hermite cubics as interpolation functions. Since the thickness varies within the element, the expression for the stiffness matrix must be integrated keeping that in mind. Assuming an element with length le, thickness t_1 in node 1, thickness t_2 in node 2 and made of a material with Young modulus E, the expression for its stiffness and geometric stiffness matrices are

$$\mathbf{K}_e = \frac{E}{60 l_e^3}\begin{bmatrix} (21t_1^3+9t_1^2t_2+9t_1t_2^2+21t_2^3) & & & \text{symmetric} \\ (15t_1^3+6t_1^2t_2+3t_1t_2^2+6t_2^3)l_e & (11t_1^3+5t_1^2t_2+2t_1t_2^2+2t_2^3)l_e^2 & & \\ (-21t_1^3-9t_1^2t_2-9t_1t_2^2-21t_2^3) & (-15t_1^3-6t_1^2t_2-3t_1t_2^2-6t_2^3)l_e & (21t_1^3+9t_1^2t_2+9t_1t_2^2+21t_2^3) & \\ (6t_1^3+3t_1^2t_2+6t_1t_2^2+15t_2^3)l_e & (4t_1^3+t_1^2t_2+t_1t_2^2+4t_2^3)l_e^2 & (-6t_1^3-3t_1^2t_2-6t_1t_2^2-15t_2^3)l_e & (2t_1^3+2t_1^2t_2+5t_1t_2^2+11t_2^3)l_e^2 \end{bmatrix}$$

$$\mathbf{K}_{Ge} = \frac{1}{30 l_e}\begin{bmatrix} 36 & & & \text{symmetric} \\ 3l_e & 4l_e^2 & & \\ -36 & -3l_e & 36 & \\ 3l_e & -l_e^2 & -3l_e & 4l_e^2 \end{bmatrix} \tag{44}$$

It can be seen from Eq. (44) that $\mathbf{K}_{Ge}$ does not depend on the element thickness as expected. The imperfection pattern selected in the simulations correspond to the buckling modes of the simply supported uniform beam, i.e.,

$$w_i^*(x) = \sqrt{\frac{2}{L}}\sin\left(\frac{i\pi x}{L}\right), \quad i = 1, 2, \ldots \tag{45}$$

The number of imperfection patterns is arbitrarily selected to 5 (m = 5) whereas 25 eigenpairs (n = 25) are extracted using the Lanczos algorithm (de Faria, 2005). The beam is discretized using 40 equal length elements and 9 thicknesses defined at nodes 1, 6, 11, 16, 21, 26, 31, 36, 41.

The optimization problem considers a constant mass constraint where the total constant mass is the mass of a uniform beam with L = 1 m, E = 70 GPa and t = 1 mm. This beam has a buckling load of λ_0 = 57.5727 N/m. Another constraint is added to the problem in order to avoid buckling loads smaller than λ_0 = 57.5727 N/m, otherwise optimal designs with excellent performance against initial imperfections but very low buckling loads could be obtained. The applied compressive loading is taken as 95% of λ_0, that is, 54.694 N/m.

Table 1 presents the uniform design and the optimal design obtained. It is observed that not only the maximum $|a_{ij}|$ decreased but also the buckling load increased. Actually, in can be seen from Eq. (11) that higher λ_i tend to decrease a_{ij}. Figure 5 gives an idea of the improvement achieved by comparing the uniform design against the optimal design.

The Plate Example

Consider a plate with variable thickness as illustrated in Fig. 6.In a similar procedure used to describe the thickness distribution in the 1D beam problem, the plate thickness distribution is piecewise linear in 2D, i.e., the thicknesses at a few nodes are specified and the thickness at the other nodes are obtained through interpolation of using the bilinear shape functions

$$N_1(\xi,\eta) = \frac{1}{4}(1-\xi)(1-\eta) \quad N_2(\xi,\eta) = \frac{1}{4}(1+\xi)(1-\eta)$$
$$N_3(\xi,\eta) = \frac{1}{4}(1-\xi)(1+\eta) \quad N_4(\xi,\eta) = \frac{1}{4}(1+\xi)(1+\eta). \tag{46}$$

Table 1. Beam optimization.

design	thickness (mm)									λ_1(N/m)	$\max_{i,j}\lvert a_{ij}\rvert$
	t_1	t_2	t_3	t_4	t_5	t_6	t_7	t_8	t_9		
uniform	1.00	1.00	1.00	1.00	1.00	1.00	1.00	1.00	1.00	57.5727	59.6
optimal	0.27	0.90	1.09	1.25	1.25	1.25	1.09	0.90	0.27	80.1951	6.55

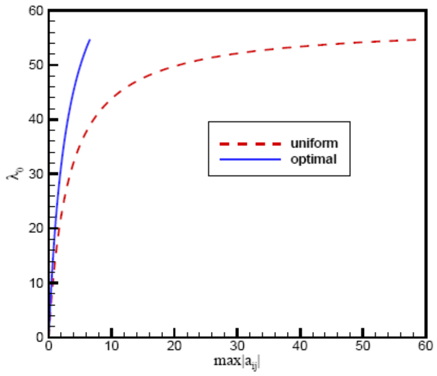

Figure 5. Uniform and optimal beam designs.

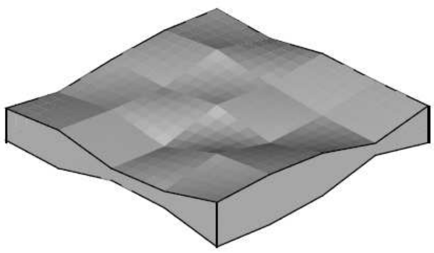

Figure 6. Representative variable thickness plate.

The finite element model employs Lagrange biquadratic elements with 9 nodes. The element formulation follows the Mindlin plate theory where each node has three degrees of freedom: one transverse displacement and two rotations. This element is prone to shear locking but in the present simulations this undesirable drawback has not been observed. Moreover, it can be conveniently avoided by reduced selective integration schemes if necessary.

The integrations required at the element level to form $\mathbf{K}_e$ and $\mathbf{K}_{Ge}$ are done numerically through Gaussian quadrature with 3 points in each local coordinate direction (ξ and η), summing up to nine integration stations.

The imperfection patterns are assumed to be sinusoidal and of the form

$$w_{i,j}^{*}(x,y)=\sqrt{\frac{4}{ab}}\sin\left(\frac{i\pi x}{a}\right)\sin\left(\frac{j\pi y}{b}\right),\quad i,j=1,2,3,4, \tag{47}$$

where a and b are the simply supported plate sides measured along x and y respectively. In the plate example a = 1.0 m and b = 1.5 m. A total of 32 eigenpairs are extracted. The thickness is defined at 15 stations, with 3 equally spaced stations in the x directions and 5 equally spaced in the y direction. However, 4 elements are used along x and 8 along y. Figure 7 shows the stations where the 15 thicknesses have been defined and the 4 × 8 mesh. Comparison against the 8 × 16 mesh shows that the 4 × 8 mesh delivers accurate results. The optimization problem considers a constant mass constraint where the total constant mass is the mass of a uniform plate with E = 70 GPa and t = 5 mm.

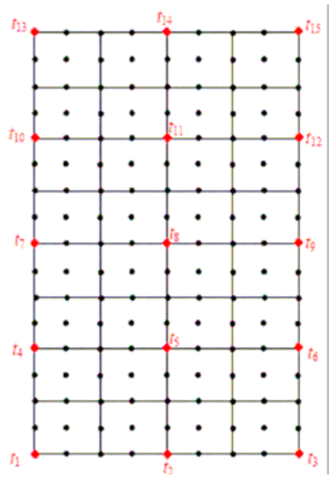

Figure 7. Plate thickness stations and mesh.

The question of selecting a suitable λ_0 is arbitrary. In the case of the simulations λ_0 is taken to be the least of the three buckling loads of the uniform plate when subjected to individual loadings R_{xx} = 1, R_{yy} = 1 and R_{xy} = 1. As in the beam example, an additional constraint is imposed to avoid designs that possess buckling loads smaller than λ_0.

Table 2 presents the uniform design and the optimal design obtained. The uniform plate has the least buckling load of 16.5 kN/m associated with R_{xx} = 1. Therefore, λ_0 = 16.5 kN/m. It is observed that not only the maximum $\|\mathbf{q}\|$ dramatically decreased but also the buckling load slightly increased. Moreover, the least λ_1 is no more associated with R_{xx} = 1 as in the uniform plate design but with R_{yy} = 1. This is evidence that the multiplicity of admissible loadings must be incorporated in the optimization search.

The optimal design is one that has no planes of symmetry (except the xy plane). If optimal designs with planes of symmetry are required for aesthetic or functional reasons then it is necessary to impose this condition in the optimization search. Interesting to notice that the beam optimal design possesses symmetry but not the plate optimal design.

Table 2. Plate optimization.

design	thickness (mm)					λ_{1xx} (kN/m)	λ_{1yy} (kN/m)	λ_{1xy} (kN/m)	max $\|\mathbf{q}\|$
	t_1 t_6 t_{11}	t_2 t_7 t_{12}	t_3 t_8 t_{13}	t_4 t_9 t_{14}	t_5 t_{10} t_{15}				
uniform	5.0 5.0 5.0	5.0 5.0 5.0	5.0 5.0 5.0	5.0 5.0 5.0	5.0 5.0 5.0	16.5	34.3	56.4	1.3×10^{7}
optimal	7.30 2.13 4.00	0.84 3.15 2.03	4.08 13.9 2.53	0.44 6.05 1.99	5.45 4.41 10.5	21.3	17.2	49.5	6.8×10^{5}

Figure 8 gives an idea of the improvement achieved by comparing the uniform design against the optimal design. The horizontal axis is normalized by the norm associated with the uniform design presented in Tab. 2 of 1.3×10^7 whereas the applied load is normalized by the λ_{1xx} of the uniform plate. In fact, the computations presented in Fig. 8 were conducted up to 95% of λ_{1xx}. A remarkable prebuckling enhancement can be observed since the equilibrium path of the optimal plate is as close to the vertical axis as it can get without violating the constraint on λ_1.

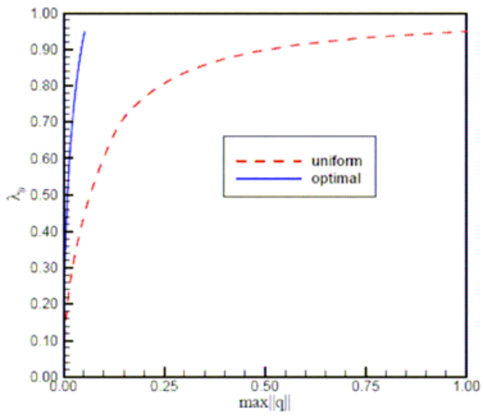

Figure 8. Uniform and optimal plate designs.

Comments and Conclusions

Two norms were proposed to measure the quality of prebuckling response of beams and plates. It was shown that the first norm, given by Eq. (6), is suitable for situations where only one load case is of interest. Since this is not a common situation encountered in practical applications, a second norm was proposed as in Eq. (24). It was further proven that both norms possess the physically intuitive property that they increase monotonically with the applied loadings.

In addition to the load case multiplicity, the realistic situation of multiple and usually unknown initial imperfection patterns is addressed. This multiplicity is represented mathematically through a convex combination of arbitrary parameters $\boldsymbol{\xi}$. Furthermore, it was proven that the proposed norms have the additional desirable property of being concave with respect to $\boldsymbol{\xi}$, what ultimately renders the twofold optimization procedure employed very efficiently. In the case of the second norm (Eq. (24)) concavity with respect to the admissible loadings is also proven. Hence, this norm has extremely desirable properties of concavity with respect to $\boldsymbol{\xi}$ and concavity with respect to the loading parameters, as long as buckling has not occurred.

When one analyzes the field of optimized thickness presented in the examples it is clear that there are some regions whose thickness is much larger than the ones found in other areas. For example, in Tab. 2, the optimized values for t_4 and t_8 are 0.44 mm and 13.9 mm, which represents a significant difference. Hence, it is clear that there are stress concentrations due to the variable nature of the thickness distribution, what could be the cause of fatigue related problems in real structures. There are two ways to overcome the stress concentration problem: (*i*) to directly include additional constraints that limit the von Mises stress levels in order to guarantee that those levels are within an acceptable range, or (*ii*) to avoid excessive thickness variation by imposing a base thickness that is constant throughout the beam or plate and, on this base structure, add a thin layer of material with variable thickness.

Two numerical examples highlight the tremendous improvement achieved in terms of prebuckling response (Figs. 5 and 8). Although applied to two simple structures, the optimization strategy presented can be used in real application where multiple load cases exist and/or uncertain imperfection patterns are present.

References

Adali, S., Richter, A. and Verijenko, V.E., 1997, “Minimum weight design of symmetric angle-ply laminates with incomplete information on initial imperfections”, *Journal of Applied Mechanics*, Vol. 64, No. 1, pp. 90-96.

Brush, D.O. & Almroth, B.O., 1975, “Buckling of Bars, Plates and Shells”, McGraw-Hill, New York.

Daniel, I.M. & Ishai, O., 2006, “Engineering Mechanics of Composite Materials”, Oxford University Press, New York.

Demjanov, V.F. and Malozemov, V.N., 1972, “Introduction to Minimax”, Moscow, Nauka.

de Faria, A.R., 2005, “Solution of buckling eigenproblems through a new variant of the Lanczos algorithm”, COBEM 2005 18th International Congress of Mechanical Engineering, 6-11 Nov., Ouro Preto, MG, Brazil.

de Faria, A.R. and Almeida, S.F.M., 2006, “The maximization of fundamental frequency of structures under arbitrary initial stress states”, *International Journal for Numerical Methods in Engineering*, Vol. 65, No.4, pp. 445-460.

de Faria, A.R. andAlmeida, S.F.M., 1999, “Enhancement of pre-buckling behavior of composite beams with geometric imperfections using piezoelectric actuators”, *Composites Part B: Engineering*, Vol. 30, No. 1, pp. 43-50.

Hansen, J.S. and Roorda, J., 1974, “On a probabilistic stability theory for imperfection sensitive structures”, *International Journal of Solids and Structures*, Vol. 10, No. 3, pp. 341-359.

Koiter, W.T., 1945, “On the Stability of Elastic Equilibrium” (in Dutch), PhD Thesis, Delf, H. J. Paris, Amsterdam. English translation, Air Force Flight Dyn. Lab. Tech., report AFFDL-TR-70-25, February, 1970.

Powell, M.J.D., 1964, “An efficient method for finding the minimum of a function of several variables without calculating derivatives”, *The Computer Journal*, Vol. 7, No. 2, pp. 155-162.

Roorda, J., 1986, “Buckling of Elastic Structures”, Solid Mechanics Division, University of Waterloo Press.

Tennyson, R.C., Chan, K.H. and Muggeridge, D.B., 1971, “The effect of axisymmetric shape imperfections on the buckling of laminated anisotropic circular cylinders”, *CASI Transactions*, Vol. 4, No. 2, pp. 131-139.

Thompson, J.M.T. & Hunt, G.W., 1973, “A General Theory of Elastic Stability”, John Wiley & Sons, London.